Caustics in turbulent aerosols

2005 Europhys. Lett. 71 186

(http://iopscience.iop.org/0295-5075/71/2/186)

EUROPHYSICS LETTERS 15 July 2005

Europhys. Lett., **71** (2), pp. 186–192 (2005)
DOI: 10.1209/epl/i2004-10532-7

Caustics in turbulent aerosols

M. Wilkinson[1] and B. Mehlig[2]

[1] *Faculty of Mathematics and Computing, The Open University Walton Hall, Milton Keynes, MK7 6AA, UK*
[2] *Department of Physics, Göteborg University - 41296 Gothenburg, Sweden*

received 29 October 2004; accepted in final form 12 May 2005
published online 10 June 2005

PACS. 05.40.-a – Fluctuation phenomena, random processes, noise, and Brownian motion.
PACS. 47.27.Qb – Turbulent diffusion.
PACS. 47.54.+r – Fluid dynamics: Pattern selection; pattern formation.

Abstract. – Networks of caustics can occur in the distribution of particles suspended in a randomly moving gas. These can facilitate coagulation of particles by bringing them into close proximity, even in cases where the trajectories do not coalesce. The evolution of these caustic patterns depends upon the Lyapunov exponents λ_1, λ_2 of the suspended particles, as well as the rate J at which particles encounter caustics. We develop a theory determining the quantities J, λ_1, λ_2 from the statistical properties of the gas flow, in the limit of short correlation times.

Aerosols are usually unstable systems, in that the suspended particles eventually coagulate. Understanding the process giving rise to this coagulation, and determining the time scale over which it occurs, are important questions in describing any aerosol system. If the gas phase does not have macroscopic motion, the coagulation may be effected by diffusion of the suspended particles, or (if the suspended particles are of a volatile substance) by Ostwald ripening. The coagulation process can be greatly accelerated if the aerosol undergoes macroscopic internal motion. Ultrasound, for example, has been used to accelerate coagulation in aerosols [1]. Turbulent flow could also play a role in the coagulation of suspended particles; this could be relevant in the coalescence of visible moisture into rain droplets [2].

If suspended particles are simply advected in an incompressible flow, their density remains constant. Inertial effects are therefore required for coagulation, unless the flow exhibits significant compressibility. In earlier work [3, 4] we discussed the motion of inertial particles experiencing viscous drag from a randomly moving fluid. Following from pioneering work by Deutsch [5], we showed that there is a phase where the trajectories of the particles coalesce, so that arbitrarily small particles coagulate. In the limit where the correlation time τ of the flow approaches zero (and probably also in the general case), this path-coalescing phase only exists when the velocity field is predominantly potential flow (such as the flow due to sound waves) [4].

Turbulent fluid flow is, however, expected to be predominantly solenoidal, and it is of interest to find alternative mechanisms of coagulation which operate outside the path-coalescence phase. Here we describe an alternative mechanism facilitating coagulation, illustrated in fig. 1: we show the distribution of particles suspended in a randomly moving gas (the equations of motion and statistics of the flow field are given by eqs. (1) to (3) below). Panel (a) shows the distribution of particles suspended in a potential flow after a short time, starting from a random scatter with uniform density. Panel (b) shows the same as (a), but for a solenoidal

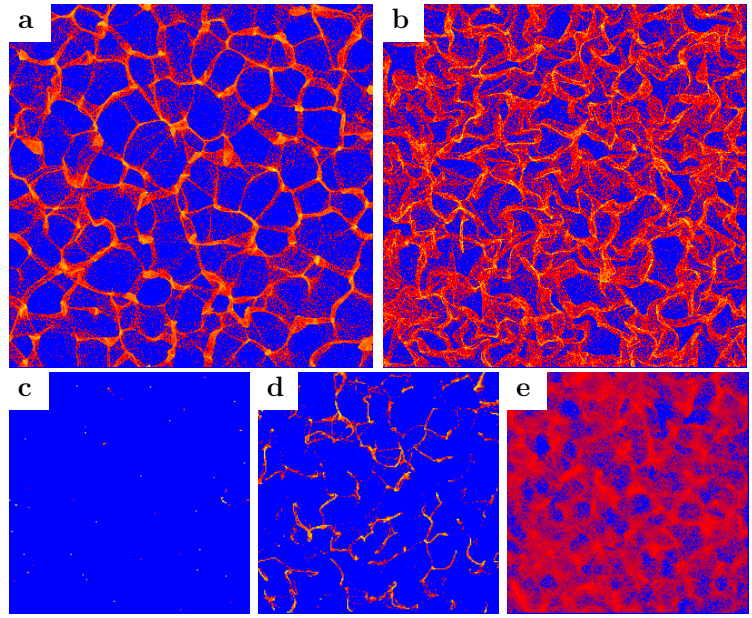

Fig. 1 – Distribution of inertial particles suspended in a randomly moving fluid (blue corresponds to lowest density, yellow to highest). The initial distribution is a random scatter. The large panels show caustics at short time, for both purely potential flow (a) and purely solenoidal flow (b). The double-line structure characteristic of caustics is more clearly visible in (a). Panels (c)-(e) show the long-time behaviour of particles in a potential flow. In all cases, the region is the unit square, the mean particle density is 2.5×10^5, $m = 1$, and the field has parameters $\xi = 0.03$, $\sigma = 0.01$, $\delta t = 0.05$, (see text). Panel (a): $\gamma = 0.53$, $t = 5$; (b): $\gamma = 0.4$, $t = 5$; (c): $\gamma = 1.18$, $t = 500$; (d): $\gamma = 0.72$, $t = 125$; (e): $\gamma = 0.21$, $t = 125$. The three small panels correspond to (c) $\lambda_2 < \lambda_1 < 0$, (d) $\lambda_1 > 0$, $\lambda_1 + \lambda_2 < 0$, and (e) $\lambda_1 > 0$, $\lambda_1 + \lambda_2 > 0$, see text.

flow. The particles cluster onto a network of caustic lines, analogous to the networks of optical caustics that can be seen on the bottom of a swimming pool [6]. This phenomenon is a new mechanism by which aerosol particles are brought into close proximity. The remaining parts of fig. 1 (c), (d), and (e) show the distribution of particles in a potential flow after a long time, in three different cases: part (c) shows the path-coalescence phase where the trajectories condense onto points. Parts (d) and (e) show two cases where there is no path coalescence, but there are significant inhomogeneities of density. In this paper we give a qualitative description of these patterns by relating the evolution of caustic patterns to the Lyapunov exponents of the particle trajectories. We remark that pictures similar to some panels of fig. 1 are displayed in various numerical investigations of particles suspended in turbulent fluids (see, for example, [7–10]) and it is surprising that the importance of caustics was not noted earlier.

Figure 1 is surprising because it is be expected that random movement of uniformly distributed particles would leave the distribution uniform. The following questions naturally arise. First, why do the particle trajectories coalesce into points in fig. 1(c)? This phenomenon was first noted in [5] and subsequently analysed in detail in [3,4] (cf. also the theory developed at the end of this letter). Secondly, why does the caustic pattern appear? We will explain why the caustics form. Third, why do the structures seen at long times (such as those in figs. 1(d) and (e)) differ? We argue that the different morphologies of the caustic patterns are related to three parameters: the rate J at which any given particle crosses caustic lines

and the Lyapunov exponents λ_1 and λ_2 of the particle trajectories (with $\lambda_1 > \lambda_2$). We present a new method for determining these parameters λ_1, λ_2, J in the limit where the correlation time of the random flow is short.

We conclude these introductory paragraphs by two remarks. The first concerns the scope of the letter. The formation of caustics causes particles to pass through regions of greatly increased density, where coagulation by contact interaction is much more likely to occur, but in this letter we confine ourselves to describing the caustics, and do not model the coagulation process. Also, because our objective is to explain the theoretical principles as clearly as possible, we confine the discussion to two spatial dimensions.

Second, there is a substantial literature concerning clustering of particles in random flows, which appeals to mechanisms which are distinct from those discussed in our present letter. Ott and Sommerer [11] proposed that, in the absence of caustics, the distribution of particles reaches a steady state with fractal density fluctuations, and with the fractal dimension related to the ratio of the Lyapunov exponents. Maxey [12] argued that particles accumulate in regions of low vorticity or high strain rate, and this approach has been extended in other works: see [13, 14] and references therein. This mechanism will be contrasted with caustic formation in the concluding paragraph of our letter.

We consider small spherical non-interacting particles of mass m, radius a, in a random flow with velocity field $\boldsymbol{u}(\boldsymbol{r}, t)$ and viscosity η. We assume that the drag force on the particles is given by Stokes's law. Neglecting displaced-mass effects, the equation of motion is

$$\ddot{\boldsymbol{r}} = -\gamma(\dot{\boldsymbol{r}} - \boldsymbol{u}), \tag{1}$$

where $\gamma = 6\pi\eta a/m$ and $\boldsymbol{r}$ is the particle position. The random driving force on the particles, $\boldsymbol{f} = m\gamma\boldsymbol{u}$, is conveniently described by two scalar potentials ϕ and ψ:

$$\boldsymbol{f}(\boldsymbol{r}, t) = \nabla\phi(\boldsymbol{r}, t) + \nabla \wedge \hat{\boldsymbol{n}}_3\psi(\boldsymbol{r}, t) \tag{2}$$

(where $\hat{\boldsymbol{n}}_3$ is a unit vector perpendicular to the plane): the scalar fields ϕ and ψ generate, respectively, the potential and solenoidal components of the flow. Here we assume that ϕ and ψ are independent, with $\langle\phi\rangle = \langle\psi\rangle = 0$ and $\langle\psi^2\rangle = \alpha^2\langle\phi^2\rangle$ for some constant α (angular brackets denote expectation values with respect to the process generating the fields ϕ and ψ). Also, we assume that the correlation function of ψ has the same form as that of ϕ:

$$\langle\phi(\boldsymbol{r} + \boldsymbol{R}, t_0 + t)\phi(\boldsymbol{r}, t_0)\rangle = C(R, t), \tag{3}$$

where $R = |\boldsymbol{R}|$, and $C(R, t)$ has correlation length ξ and correlation time τ. The theory is readily extended to more general statistics. Purely solenoidal flow is a good model for particles suspended in a turbulent fluid, when the velocity of the fluid is small compared to its speed of sound. The case of potential flow is a good model for particles suspended in a gas which is subjected to high-intensity ultrasonic noise. The intermediate case (where α is neither very large nor very small) is considered because of the mathematical insight provided by being able to interpolate between the limiting cases.

Our two-dimensional numerical simulations are performed in the limit of small τ, using a model discretised in time with a small time step $\delta t \gg \tau$: the impulse

$$\boldsymbol{f}_n(\boldsymbol{r}) = \int_{n\delta t}^{(n+1)\delta t} \mathrm{d}t' \; \boldsymbol{f}(\boldsymbol{r}_{t'}, t') \tag{4}$$

at time $n\,\delta t$ is taken to be of the form (2) in terms of scalar fields $\phi_n(\boldsymbol{r})$ and $\psi_n(\boldsymbol{r})$, satisfying $\langle\phi_n(\boldsymbol{r})\phi_{n'}(\boldsymbol{r}')\rangle = \sigma^2\,\xi^2\,\delta t\,\exp[-|\boldsymbol{r} - \boldsymbol{r}'|^2/2\xi^2]\delta_{nn'}$ and $\langle\psi_n(\boldsymbol{r})\psi_{n'}(\boldsymbol{r}')\rangle = \alpha^2\langle\phi_n(\boldsymbol{r})\phi_{n'}(\boldsymbol{r}')\rangle$.

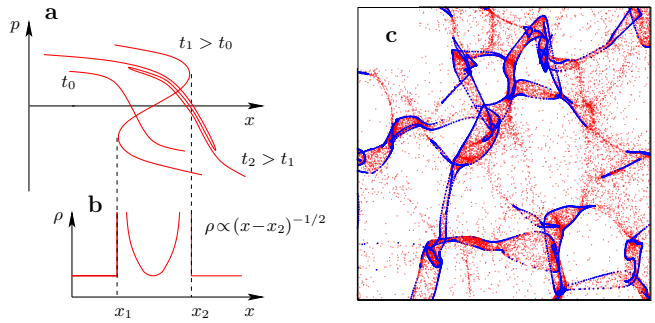

Fig. 2 – (a) Particles are assumed to be distributed on a phase-space manifold, shown here as a phase curve in a one-dimensional section. The phase curve develops folds (at time t_1), which become flattened due to the effect of damping (at t_2). (b) The particle density at time t_1 diverges on caustics, which are the projections of the folds. The caustics are created in pairs, with a high density of particles between each pair. (c) The particle distribution is shown in red, and the corresponding caustic curves are plotted as blue lines. The parameters are the same as for fig. 1(a).

The origin of the caustics is most easily understood by a one-dimensional example. Figure 2(a) is a schematic plot of the momentum p of a particle as a function of its position x. We assume that at time $t_0 = 0$, this is a single-valued function, but at a later time this function may develop a pair of folds because the faster particles overtake the slower ones. If the density of particles is smoothly distributed along the line in phase-space, the projected density in coordinate space at time t_1, shown in part (b), is singular at a pair of caustics, which are the projections of each fold. We see that the caustics are created in pairs, and that initially there is a high density of particles between the caustic lines, as well as a divergent density on the

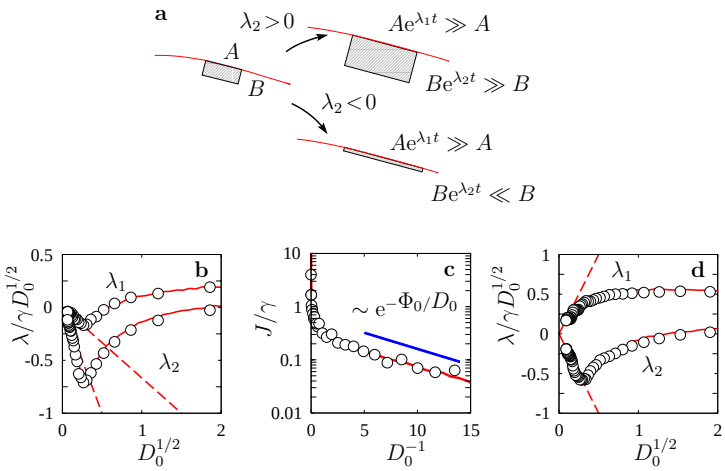

Fig. 3 – (a) The Lyapunov exponents λ_1 and λ_2 determine the evolution of the caustic pattern. (b) Lyapunov exponents λ_1 and λ_2 for $\Gamma = 1/3$; simulations of Langevin equations (lines) and integration of equation of motion (○). Also shown are the asymptotes for small $D_0^{1/2}$ (see text). (c) Corresponding rate of crossing caustics. (d) Same as (b), but for $\Gamma = 3$.

caustic itself. The damping term (with coefficient γ in eq. (1)) implies that momentum differences decrease, so that the caustics become progressively more sharply folded, as illustrated for $t_2 > t_1$ in fig. 2(a). Figure 2(c) shows a segment of the actual caustic pattern. The caustic lines cannot abruptly end, but caustics can join at cusps [6], some of which are visible in the figure. Some regions of high density do not have an associated pair of caustic lines. This is because the phase-space manifold is nearly perpendicular to the coordinate-space plane, but it has not yet folded over. At short times, our caustic networks are equivalent to the lines of bright light observed on the bottom of a swimming pool on a sunny day when the water surface is disturbed. The morphology of the swimming-pool caustics is discussed by Berry [6].

The examples in fig. 1 show that the morphology of the patterns depends upon the statistics of the random velocity field. It is desirable to understand the differences between these figures. To this end we consider the behaviour of three particles, a reference particle and two nearby ones separated by $\delta\boldsymbol{r}$ and $\delta\boldsymbol{r}'$. The evolution of these small increments is described by the Lyapunov exponents, λ_1 and λ_2, characterising the time dependence of the length $X(t) = |\delta\boldsymbol{r}(t)|$ of one of the separation vectors, and of the area of a parallelogram spanned by two vectors, $A(t) = |\delta\boldsymbol{r}(t) \wedge \delta\boldsymbol{r}'(t)|$. These are defined by

$$\lambda_1 = \lim_{t\to\infty} \frac{1}{t} \log_{\mathrm{e}} \left| \frac{X(t)}{X(0)} \right|, \qquad \lambda_1 + \lambda_2 = \lim_{t\to\infty} \frac{1}{t} \log_{\mathrm{e}} \left| \frac{A(t)}{A(0)} \right|. \tag{5}$$

Now we use the Lyapunov exponents to gain an understanding of the caustic patterns in figs. 1(d), (e). When $\lambda_1 < 0$, almost all infinitesimal line segments contract to a point, and the trajectories of particles coalesce as shown in fig. 1(c). This was the principle used to explain the coalescence transition, discussed in [3] and [4]. Next, consider what happens if λ_1 is positive, so that the trajectories do not coalesce into points. In this case, we consider a small element of area on a caustic line, extended in the direction of the caustic (fig. 3(a)). This element is expected to be stretched along the direction of the caustic, because we assume $\lambda_1 > 0$. If λ_2 is also positive, the line width of the element will also expand in the direction perpendicular to the caustic, and the density fluctuation resulting from the caustic becomes weaker as time proceeds: this is illustrated by fig. 1(e). If $\lambda_2 < 0$, the line element contracts in the direction perpendicular to the caustic, and if in addition $\lambda_1 + \lambda_2 < 0$, the concentration of particles on the caustic increases. This case is illustrated by fig. 1(d), which shows very narrow caustic lines. The increase in particle density on the caustic lines cannot proceed without limit: the caustic line stretches and folds, until the particles aligned along the caustic have become indistinguishable from points randomly scattered in the plane. In this case, the caustic also disappears, although this happens more slowly than when $\lambda_1 + \lambda_2 > 0$. The fold lines in the phase-space manifold persist forever, but we have argued that their physical manifestation in the distribution of particles becomes less pronounced, so that each caustic only influences the particle distribution for a finite time. However, new caustics are created at a uniform rate, described by the rate constant J.

We will now show how the three parameters λ_1, λ_2 and J may be determined quantitatively. The most complete results are available in the limit where the correlation time τ is very short. We linearise eq. (1), and obtain $\delta\dot{\boldsymbol{r}} = \delta\boldsymbol{p}/m$, $\delta\dot{\boldsymbol{p}} = -\gamma\delta\boldsymbol{p} + \mathbf{F}(t)\delta\boldsymbol{r}$, where $\mathbf{F}$ is a matrix with elements $F_{ij}(t) = \partial f_i(\boldsymbol{r}(t), t)/\partial r_j$. Consider now the motion of three particles, one reference particle and two nearby ones, separated by $(\delta\boldsymbol{r}, \delta\boldsymbol{p})$ and $(\delta\boldsymbol{r}', \delta\boldsymbol{p}')$ from the reference trajectory. The angle $\delta\varphi$ separating the vectors $\delta\boldsymbol{r}$ and $\delta\boldsymbol{r}'$ is very small, and the lengths of these vectors, X and X' respectively, are initially equal. We also assume that the vectors $\delta\boldsymbol{p}$ and $\delta\boldsymbol{p}'$ are initially separated by a small angle, of order $\delta\varphi$. We now make a change of coordinates from

$\delta\boldsymbol{r}$, $\delta\boldsymbol{p}$, $\delta\boldsymbol{r}'$, $\delta\boldsymbol{p}'$ to the set X, X', θ, $\delta\varphi$, Y_1, Y_2, Z_1, Z_2:

$$\begin{aligned} \delta\boldsymbol{r} = X\hat{\boldsymbol{n}}_\theta\,, \qquad & \delta\boldsymbol{r}' \;=\; X'\hat{\boldsymbol{n}}_{\theta+\delta\varphi} \\ \delta\boldsymbol{p} = X(Y_1\hat{\boldsymbol{n}}_\theta + Y_2\hat{\boldsymbol{n}}_{\theta+\pi/2}), \qquad & \delta\boldsymbol{p}' \;=\; X'\big[(Y_1+Z_1\delta\varphi)\hat{\boldsymbol{n}}_{\theta+\delta\varphi} + (Y_2+Z_2\delta\varphi)\hat{\boldsymbol{n}}_{\theta+\frac{\pi}{2}+\delta\varphi}\big] \end{aligned} \tag{6}$$

($\hat{\boldsymbol{n}}_\theta$ denotes a unit vector in two dimensions with direction θ). We expect that X may increase or decrease, $\delta\varphi$ decreases with probability one (because random linear mapping of any two vectors results in vectors becoming aligned), X'/X remains close to unity, θ will become uniformly distributed on $[0, 2\pi]$, and that Y_1, Y_2, Z_1 and Z_2 approach a stationary distribution. The length of a vector separating two nearby points is X, so that $\lambda_1 = \langle \dot{X}/X\rangle$. The area spanned by the two vectors is $\delta A \sim XX'\delta\varphi \sim X^2\delta\varphi$, so that $\lambda_2 + \lambda_1 = \langle \delta\dot{\varphi}/\varphi\rangle + 2\langle \dot{X}/X\rangle$ (here we used the fact that $\delta\varphi \ll 1$). We find the equations of motion for these variables. For X and $\delta\varphi$ we find $\dot{X} = Y_1X/m$ and $\delta\dot{\varphi} = Z_2\delta\varphi/m$, so that the Lyapunov exponents are

$$\lambda_1 = \langle Y_1\rangle/m, \qquad \lambda_2 = \lambda_1 + \langle Z_2\rangle/m. \tag{7}$$

For θ, we find $\dot{\theta} = Y_2/m$, and conclude that θ becomes uniform on $[0, 2\pi]$ as implied by rotational invariance. For the remaining variables we find the following equations, where $\hat{\boldsymbol{n}}_1 = \hat{\boldsymbol{n}}_\theta$, $\hat{\boldsymbol{n}}_2 = \hat{\boldsymbol{n}}_{\theta+\pi/2}$, $F'_{ij}(t) = \hat{\boldsymbol{n}}_i \cdot \mathbf{F}(t)\hat{\boldsymbol{n}}_j$:

$$\begin{aligned} \dot{Y}_1 &= -\gamma Y_1 + \big(Y_2^2 - Y_1^2\big)/m + F'_{11}\,, \\ \dot{Y}_2 &= -\gamma Y_2 - 2Y_1Y_2/m + F'_{21}\,, \\ \dot{Z}_1 &= -\gamma Z_1 - 2\big(Z_1Z_2/2 + Y_1Z_1 - Y_2Z_2\big)/m + F'_{21} + F'_{12}\,, \\ \dot{Z}_2 &= -\gamma Z_2 - 2\big(Z_2^2/2 + Y_1Z_2 + Y_2Z_1\big)/m - F'_{11} + F'_{22}\,. \end{aligned} \tag{8}$$

In the limit where the correlation time of the random velocity field is short, we can approximate eqs. (8) by a set of coupled Langevin equations. We write these in a dimensionless form by introducing dimensionless variables x_i, such that $(Y_1, Y_2, Z_1, Z_2) = m\gamma(x_1, x_2, x_3, x_4) \equiv m\gamma\boldsymbol{x}$, $t' = \gamma t$ and find

$$\mathrm{d}\boldsymbol{x} = \boldsymbol{v}(\boldsymbol{x})\mathrm{d}t' + \mathrm{d}\boldsymbol{w}, \tag{9}$$

where $v_1 = -x_1 + (x_2^2 - x_1^2)$, $v_2 = -x_2 - 2x_1x_2$, $v_3 = -x_3 - x_3x_4 - 2(x_1x_3 - x_2x_4)$, $v_4 = -x_4 - x_4^2 - 2(x_1x_4 + x_2x_3)$, $\langle \mathrm{d}w_i\rangle = 0$, $\langle \mathrm{d}w_i\,\mathrm{d}w_j\rangle = 2D_{ij}\,\mathrm{d}t'$. The diffusion matrix with elements D_{ij} is

$$\mathbf{D} = D_0 \begin{pmatrix} 1 & 0 & 0 & -(\Gamma+1)/2 \\ 0 & \Gamma & (\Gamma+1)/2 & 0 \\ 0 & (\Gamma+1)/2 & \Gamma+1 & 0 \\ -(\Gamma+1)/2 & 0 & 0 & \Gamma+1 \end{pmatrix}, \tag{10}$$

where

$$D_0 = \frac{1}{2m^2\gamma^3}\int_{-\infty}^{\infty} \mathrm{d}t\ \langle F_{11}(t)F_{11}(0)\rangle, \qquad \Gamma = \frac{1+3\alpha^2}{3+\alpha^2} \tag{11}$$

(we used rotational invariance to conclude that the statistics of F'_{ij} are identical to those of F_{ij}). In our simulations, $D_0 = (3+\alpha^2)\sigma^2/(2m^2\gamma^3\xi^2)$. The three parameters describing caustic formation are obtained from the stationary state of the Langevin process (9): the rate J at which a representative particle passes through a caustic is the same as the frequency with which the area of the parallelogram spanning the two vectors $\boldsymbol{r}$ and $\boldsymbol{r}'$ becomes equal to zero, or, equivalently, the rate at which $\delta\varphi$ passes through zero. An equivalent condition

is that the trajectory in the (Z_1, Z_2)-plane goes to infinity (reappearing from the reflected direction): $J = \gamma j$, where j is the rate at which x_4 escapes to infinity. Figures 3(b) and (d) show comparisons between a direct evaluation of the Lyapunov exponents (using a method described in [15]), and simulations using eq. (9), for $\Gamma = 1/3$ and $\Gamma = 3$. Also shown are the asymptotes for small $D_0^{1/2}$, namely $\lambda_1/\gamma = (\Gamma - 1)D_0$ and $\lambda_2/\gamma = -2D_0$. These results for the asymptotes are equivalent to those derived in [16,17] for advected particles.

Equation (9) is equivalent to a Fokker-Planck equation for the distribution $P(\boldsymbol{x}, t)$, namely $\partial P/\partial t' = \nabla \cdot [-\boldsymbol{v}P + \mathbf{D}\nabla P]$. Considering a steady-state solution in the limit $D_0 \to 0$, we find that a WKB ansatz, of the form $P(\boldsymbol{x}) = \exp[-\Phi(\boldsymbol{x})/D_0]$, is appropriate. We therefore expect that the escape current vanishes exponentially as $D_0 \to 0$, being of the form $j \sim j_0 \exp[-\Phi_0/D_0]$ (where j_0 may have an algebraic dependence on D_0). Figure 3(c) shows that the caustic formation rate does vanish exponentially as $D_0 \to 0$, with action $\Phi_0 \approx 0.14$.

In this letter we have shown that caustics can be a mechanism for the clustering of particles suspended in a random flow, in cases where the inertia of the particles is significant. This mechanism differs from that considered by Maxey [12], in that it is both more general and more powerful. The mechanism introduced in [12] is only effective when the damping rate γ and the correlation time τ of the velocity field satisfy $\gamma\tau \sim 1$, whereas caustics can occur even when $\gamma\tau \ll 1$ (all of the numerical examples in this letter are relevant to that case). Also, caustics can cause an unbounded increase of the density of particles after a finite time, which is not possible in the approach described in [12–14]. We have also introduced a new method for determining both of the Lyapunov exponents for the particle flow in two spatial dimensions from expectation values of a Langevin process. This method can be used to derive an efficient perturbative expansion for the Lyapunov exponents, and can also be adapted to higher-dimensional systems.

Note added in proofs. – We learned that Falkovich *et al.* have suggested that caustics may play a part in the clustering of aerosol particles: see Falkovich G., Fouxon A. and Stepanov M. G., *Nature*, **419** (2002) 151.

REFERENCES

[1] Gooberman G. L., *Ultrasonics: Theory and Application* (Hart Publications, New York) 1969.
[2] Shaw R. A., *Annu. Rev. Fluid Mech.*, **35** (2003) 183.
[3] Wilkinson M. and Mehlig B., *Phys. Rev. E*, **68** (2003) 040101.
[4] Mehlig B. and Wilkinson M., *Phys. Rev. Lett.*, **92** (2004) 250602.
[5] Deutsch J., *J. Phys. A*, **18** (1985) 1457.
[6] Berry M. V., *Singularities in Waves, Les Houches Lecture Series Session XXXV*, edited by Balian R., Kléman M. and Poirier J.-P. (North Holland, Amsterdam) 1981, pp. 453-543.
[7] Sigurgeirsson H. and Stuart A. M., *Phys. Fluids*, **14** (2002) 4352.
[8] Bec J., *Phys. Fluids*, **15** (2003) L81.
[9] Boffetta C., De Lillo F. and Gamba A., *Phys. Fluids*, **16** (2004) L20.
[10] Bec J., Celani A., Cencini M. and Mussacchio S., preprint: nlin. CD/0407013.
[11] Ott E. and Sommerer J., *Science*, **359** (1993) 334.
[12] Maxey M. R., *J. Fluid. Mech.*, **174** (1987) 441.
[13] Elperin T., Kleeorin N. and Rogachevskii I., *Phys. Rev. Lett.*, **77** (1996) 5373.
[14] Balkovsky E., Falkovich G. and Fouxon A., *Phys. Rev. Lett.*, **86** (2003) 2790.
[15] Eckmann J. P. and Ruelle D., *Rev. Mod. Phys.*, **57** (1985) 617.
[16] Baxendale P. and Harris T., *Ann. Probab.*, **14** (1986) 1155.
[17] Klyatskin V. I. and Gurarie D., *Phys. Usp.*, **42** (1999) 165.